AECL-6883

ATOMIC ENERGY OF CANADA LIMITED

L'ÉNERGIE ATOMIQUE DU CANADA LIMITÉE

THE EFFECT OF THERMAL CYCLING ON THE MOVEMENT OF THE α Zr/ α Zr + HYDRIDE PHASE BOUNDARY IN COLD-WORKED Zr-2.5 wt% Nb ALLOY

Effet de cyclage thermique sur le mouvement de la couche limite de phases α Zr/ α Zr + hydrure dans l'alliage écroui Zr-2.5% pds Nb

B. COX and V.C. LING

Chalk River Nuclear Laboratories Laboratoires nucléaires de Chalk River

Chalk River, Ontario

May 1980 mai

ATOMIC ENERGY OF CANADA LIMITED

THE EFFECT OF THERMAL CYCLING ON THE MOVEMENT OF THE αZr/αZr+HYDRIDE PHASE BOUNDARY IN COLD-WORKED Zr-2.5 wt% Nb ALLOY

by

B. Cox and V.C. Ling

Chalk River Nuclear Laboratories
Chalk River, Ontario K0J 1J0
May 1980

AECL-6883

L'Energie Atomique du Canada, Limitée

Effet de cyclage thermique sur le mouvement de la couche limite de phases $\alpha Zr/\alpha Zr$ + hydrure dans l'alliage écroui Zr-2.5% pds Nb

par

B. Cox et V.C. Ling

Résumé

Une section de tube de force en alliage écroui Zr-2.5% pds Nb a été hydrurée à une extrémité dans une solution LiOH de 40 g/L à 573 K (cette extrémité ayant été précédemment nickelée). Il en a resulté une couche massive d'hydrure de 0.6 mm d'épaisseur plus ∿130 ppm d'hydrogène dans le centre sous la plaque de nickel. Un cyclage thermique, effectué dans des conditions semblables à celles susceptibles de se produire lors de l'arrêt lent d'un réacteur n'a pas provoqué de mouvement significatif de la couche limite de phases α + hydrure/α le long du tube jusqu'à 2688 cycles de 573 à 523 K. On a remarqué la surcompression du centre dans la partie nickelée. On a pu tirer quelques conclusions en ce qui concerne l'origine de l'hydrogène dans la partie nickelée et les facteurs contrôlant le processus de surcompression.

Laboratoires nucléaires de Chalk River
Chalk River, Ontario K0J 1J0

Mai 1980

AECL-6883

ATOMIC ENERGY OF CANADA LIMITED

THE EFFECT OF THERMAL CYCLING ON THE MOVEMENT OF THE αZr/αZr+HYDRIDE PHASE BOUNDARY IN COLD-WORKED Zr-2.5 wt% Nb ALLOY

by

B. Cox and V.C. Ling

ABSTRACT

A piece of CW Zr-2.5 wt% Nb alloy pressure tube was hydrided at one end in 40 g/L LiOH solution at 573 K (after nickel-plating that end). The result was a solid hydride layer 0.6 mm thick plus $\sim$ 130 ppm hydrogen in the core under the nickel plate. Thermal cycling under conditions similar to those likely to be experienced during a reactor trip did not cause any significant movement of the α+hydride/α phase boundary along the tube for up to 2688 cycles from 573 to 523 K. Supercharging of the core was observed in the nickel-plated area. Some conclusions have been drawn concerning the origin of the hydrogen in the nickel-plated area, and the factors controlling the supercharging process.

Chalk River Nuclear Laboratories
Chalk River, Ontario K0J 1J0
May 1980

AECL-6883

1. INTRODUCTION

When hydrogen is absorbed rapidly into a zirconium alloy specimen, the result is often a crust of solid zirconium hydride around the αZr core. When the specimen is held for times long enough to eliminate concentration gradients in the core this should contain hydrogen equivalent to the solubility in zirconium at the highest temperature attained during hydrogen absorption, or the as-received hydrogen content of the material, whichever is the higher [1].

Observation shows that if the specimen is thermally cycled during (or after) the hydrogen absorption process, or if the hydrogen is absorbed slowly during corrosion, the hydrogen content of the core may exceed the solubility at the highest temperature seen by the specimen [2]. This "supercharging" effect may be observed whether or not a solid hydride crust is formed at some time during the experiment [2-9], and the thermal cycling effect is commonly used to homogenize specimens in which it is desired to achieve a high hydrogen content by (e.g.) gaseous hydriding [9] or corrosion in concentrated LiOH solution [8,10].

The mechanism of this "supercharging" has been discussed by several authors, but no single explanation is yet completely accepted [2-7]. There are two main opposing hypotheses; the first, which applies to the isothermal situation during corrosion and was proposed by Marino [4], argues that when the flux of hydrogen into the specimen is low, the supercharging results from the ability of the system to maintain a small degree of supersaturation (and hence a concentration gradient) in the presence of precipitated hydride. The second, proposed by Westlake [6], applies primarily to thermally cycled specimens, and derives from the well-known hysteresis between the dissolution and precipitation processes for zirconium hydrides [11] coupled with the very rapid diffusion of hydrogen in α-Zr at relatively low temperatures ($< 0.3\ T_m$)[12]. This would permit further diffusion of hydrogen into the core of a specimen during any period when the α-Zr core is unsaturated in hydrogen by virtue of the hysteresis in the dissolution process during the heating part of a thermal cycle. It should be pointed out that there is much evidence that thermal cycling is not a prerequisite for supercharging [7], so it seems most probable that both mechanisms are capable of operating given the right combination of conditions. It was hoped that this work would shed some light on this question, but this was not the primary intent of the study.

The purpose of this study was to investigate the magnitude and range over which the supercharging effect is operative, but not to attempt a final distinction between competing hypotheses. Most specimens used in studies of "supercharging" have been taken from material of relatively thin section (≤ 4.5 mm), so that, with access for hydrogen to both faces, the distance over which "supercharging" was observed was comparable to the diffusion distance for

hydrogen in α-Zr for the time and temperature profile of a single thermal cycle. A situation may arise in a CANDU reactor pressure tube where a hydrogen concentration gradient exists along the length of the tube [13]. It was of interest to learn whether, under conditions where an α/α+hydride phase boundary occurs within this concentration gradient, thermal cycling will or will not accelerate the motion of this phase boundary along the tube. The results of a series of experiments to examine this question are presented here.

2. EXPERIMENTAL

A partially tubular specimen 15.2 cm (6 inches) long by 3.81 cm (1.5 inch) wide was cut from a cold-worked (CW) Zr-2.5 wt% Nb pressure tube (Identification No.929). The specimen was pickled in a standard nitric/hydrofluoric/sulphuric acid mixture, and 5.08 cm (2 inches) at one end was nickel-plated (on the outside of the partial tube). It was known from previous experience [14] that, unlike Zircaloy-2, it was necessary to provide a "hydrogen-window" in order to get high hydrogen uptakes in Zr-2.5 wt% Nb during corrosion in LiOH. Even with one end nickel-plated, the first two attempts to hydride the specimen failed, and hydriding was eventually achieved by M.C. Teeter, Hawker-Siddeley of Canada, Orenda Division. An exposure of 5 days at 573 K (300°C) to 40 g/L LiOH without thermal cycling was desired. In practice, one brief thermal cycle was experienced after 10.5 hours autoclaving.

The specimen was cut into five longitudinal strips. One of these was first metallographically polished along one long edge, photographed, and then cut into 0.25 cm pieces for hydrogen analysis.

Three strips were given, respectively, 336 cycles between 473 and 573 K (∿ 200 and 300°C)(Figure 1a); 672 cycles between ∿ 523 and 573 K (∿ 250 and 300°C) and 2688 cycles between ∿ 523 and 573 K (∿ 250 and 300°C) (Figure 1b), in laboratory air. The thermal cycle between 573 and 523 K (300 and 250°C) approximates that seen by the outlet end of a CANDU fuel channel each time there is a reactor trip. Each of these three specimens was then polished metallographically along one edge, photographed, and sectioned for hydrogen analysis. The hydrogen analyses were performed by General Chemistry Branch, CRNL, using a LECO (RD-1) gas analyzer.

The final strip has been used to prepare samples for X-ray analysis.

3. RESULTS

After autoclaving the nickel plating remained adherent over most of the plated area, with a thin dark tarnish film over much of its surface. The remainder of the surface was covered with a

streaky white oxide, with the streaks aligned in the extrusion direction. Small areas where the nickel plating had not adhered also showed white oxide. Thicker white oxide was evident on specimen edges and corners. When the nickel plating was stripped from adherent areas the Zr-Nb surface below was black, this was thought to indicate the pre-plating surface preparation rather than the presence of a black oxide film. Metallography showed (Figure 2) that the uniform white oxide film was about 6-10 μm thick, with patches up to 70 μm at edges, and that there was no visible oxide in the area covered by the nickel plating.

Although the time and temperature of exposure were based [14] on a desire to achieve 200 ppm of uniformly distributed hydride in the plated end of the specimen, metallography (Figure 3) showed that a solid hydride layer was present beneath the nickel plating. X-ray analysis showed it to be γ-ZrH. This layer tapered to zero at the boundary of the nickel plating (Figure 4) and was a fairly uniform 0.6 mm thick over most of the plated area, with a diffuse zone of two phase ($\alpha+\gamma$) material extending a further 0.4 mm (Figure 3). Beneath the hydride layer a uniform α+hydride region containing a low hydrogen content (Figure 4) extended across the remaining 3 mm of the wall thickness. This relatively uniform α+hydride region showed a gradient of decreasing hydride precipitate volume in the vicinity of the end of the nickel plating.

The volume percent of hydride phase was estimated from metallographs taken along the centre-line of the specimen at intervals. Inspection showed that (with the exception of the area immediately adjacent to the solid hydride boundary) the volume fraction was macroscopically uniform across any section of the specimen, although there was a tendency for banding of the hydride to occur. The results for the metallographic estimates of hydride volume fraction along the centre-line of each specimen are listed in Table 1 and plotted in Figure 5. The hydrogen analyses obtained by the inert gas fusion method are tabulated in Table 2 and plotted in Figure 6 for those specimens not including any solid hydride. The metallographic estimates of hydride volume fraction and the corresponding hydrogen analyses given in these figures and tables were kept in registry with each other by reference to the end of the nickel plating. Metallography on all four specimens is compared in Figure 7 at the peak hydrogen point on the specimen centre-line and in Figure 8 at points beyond the diffusion profile.

4. DISCUSSION

4.1 Corrosion and Hydriding of Zr-2.5% Nb in LiOH

The corrosion and hydriding of the Zircaloys in concentrated LiOH solutions has been known for many years [15], and appears to occur regularly and reproducibly with a roughly constant $\sim$ 65% of the hydrogen released by the corrosion process at 573 K (300°C)

finishing in the metal phase [8]. The behaviour of the Zr-2.5% Nb alloy is similar as regards corrosion rate, thick white oxide films are rapidly formed [14]. However, the percentage of corrosion hydrogen absorbed is much less than for the Zircaloys, being reported at about 6% [14] during corrosion at 633 K (360°C).

In order to use the LiOH method for controlled hydriding of Zr-2.5% Nb specimens, in the same manner as it has been used for the Zircaloys, the expedient of nickel-plating one surface to act as a hydrogen window has been used [14]. Problems with adherence of the nickel plating have been frequent, but even with good adherence of the plating irreproducibility seems to be a feature of the use of this method for Zr-2.5% Nb. Thus, in this experiment, the oxide thickness on the unplated areas of the specimen varied from 8-10 μm (≡ 120-150 mg/dm^2) on much of the surface, with some thicker patches, to > 50 μm at edges. Eight micrometres is about thickness of oxide expected for Zircaloys exposed to 40 g/L LiOH at 573 K (300°C) for 5 days [8]. The hydrogen absorption (in areas away from the nickel plating) of 3.5 ppm was, however, smaller than anticipated [14]; being equivalent to only ∿ 4% of the corrosion hydrogen. During the subsequent thermal cycling in laboratory air, however, the hydrogen uptake was higher than expected, considering that hydrogen uptake in moist air by Zr-2.5% Nb is usually very low [16]. Perhaps a high oxidation rate persisted in air after exposure to LiOH, however, no check was made on this.

In the nickel-plated area the averaged hydrogen content seems to have been about 1400 μg/g. An 0.6 mm thick γ-ZrH layer should average out to ∿ 1600 μg/g. On many samples flaking of the solid hydride layer was observed during extraction from the mount after metallography and during cutting for analysis. This would result in much lower analytical values than expected, and it may be that there was some flaking on all specimens even though it may have escaped notice. The average hydrogen content was much higher than expected [14], and corresponds to ≥ 300% of the corrosion hydrogen released by the whole specimen. Thus, a source of hydrogen other than the corroding Zr-Nb surface must have been present.

The irreproducibility of the hydrogen absorption process is shown by a comparison with the pressure-tube sample (used as the pressure vessel for the experiment) which was nickel-plated on the side exposed to LiOH (inside), and absorbed an average of 50-60 μg/g [17], and with other small specimens [18], nickel-plated over half their surface area (one side), which showed oxide thicknesses of ∿ 8 μm on the unplated area, hydride layers 0.6 mm thick on areas where contact with the nickel plating was maintained, and central hydrogen contents comparable to the large specimen (Figure 9). Our sample and the above specimens were plated by the same technique, at the same time, and were exposed to the same LiOH solution as each other.

The question which immediately arises is the source of the hydrogen absorbed in the nickel-plated areas. Price [14] gives his opinion that this arises from corrosion of the nickel plating. If this were the source, then one might have expected all the specimens to have absorbed similar amounts of hydrogen, since the nickel on each specimen, being similar, should have corroded to the same extent. In addition, there were few visible signs of any extensive corrosion or etching of the nickel plate, only a thin tarnish film was present.

A study of the nature of the irreproducibility between specimens suggested the correlation that the amount of hydrogen absorbed was inversely proportional to the fraction of the exposed Zr-Nb alloy surface which was nickel-plated. The conclusion one might reach from this is that if a specimen could be completely nickel-plated, to give a completely non-porous coating, then in the absence of hydrogen added to the water (or some other source of hydrogen such as corrosion of other parts of the system) there should be effectively no hydrogen absorbed by the specimen. This situation is approximated by the pressure tube (nickel-plated on its inner surface) where the only source of hydrogen would be small defective areas on the plating (possibly at tube ends), other corroding specimens in the same system, or corrosion of external steel components in the system. For the other specimens present the amount of hydrogen absorbed through the nickel plating seems to be more than that equivalent to the corrosion hydrogen released by the corrosion of the unplated area of the specimen.

This hydrogen could be getting into the specimen by several methods.

(i) The corrosion hydrogen from the oxidation of unplated areas of zirconium alloy could contribute to the total dissolved hydrogen in the LiOH, and from there be absorbed through the nickel plating, acting simply as a window.

(ii) The cathodic portion of the zirconium corrosion reaction (i.e. the discharging of protons at the metal surface by the emerging electrons) could be occurring entirely on the nickel plating, which, by acting as a window, could lead to the absorption of hydrogen equivalent to (but not greater than) 100% of that released by corrosion on the total unplated area.

(iii) The galvanic couple between nickel and zirconium might result in the cathodic release of hydrogen at the nickel surface, which because of the poor ability of nickel to recombine nascent hydrogen could be absorbed through the plating rather than released as hydrogen gas into the LiOH solution.

(iv) The hydrogen could come from corrosion of the nickel.

These possibilities can be distinguished by the following reasoning. If (i) were the mechanism, then by virtue of the similar nickel plating on all specimens in the same experiment, and the averaging effect of the hydrogen dissolving in the circulating LiOH, all specimens should show the same rate of hydrogen absorption per unit area of plating. This is not the case. Routes (ii) and (iii) should both give effects dependent on anode to cathode area ratio. However, a distinction can be made because if (ii) is operating then the total amount of hydrogen absorbed by a partially plated specimen should not exceed that equivalent to the total amount of oxidation, whereas if (iii) were operating then the total hydrogen absorbed could exceed that equivalent to the amount of corrosion occurring provided that a "non-corrosive" anodic reaction (e.g. oxidation of OH^-) were available at the zirconium alloy surface. The most telling evidence for eliminating (ii) is the observation that the total hydrogen absorbed exceeded 100% of that available from the zirconium corrosion process. Since there appeared to have been little corrosion of the nickel plating, which could have supplied the necessary hydrogen or made up the difference between that available by route (ii) and that found analytically, route (iv) can also be eliminated. In this experiment, the hydrogen absorbed by the specimen was > 300% of the equivalent corrosion hydrogen, which seems to be so far outside the possible limits of error based on variations in oxide thickness that the excess is unlikely to have resulted from the apparently small extent of nickel corrosion. Thus, we conclude that a galvanic couple between Zr-Nb and Ni (mechanism (iii)) was the most probable source of the hydrogen. In the other specimens in the same experiment, the different anode/cathode area ratios and hydrogen uptakes are in approximate agreement with such an hypothesis, when allowance is made for the imperfect adhesion of the nickel to the small specimens.

4.2 Hydrogen Distributions

(a) In nickel-plated area

The area under the nickel plating after corrosion in LiOH showed a solid hydride layer 0.6 mm thick, a diffuse hydride layer a further 0.4 mm thick, and a relatively uniform distribution of hydride platelets over the rest of the specimen core which analyzed at an average of 130 ppm. The hydrogen content of the core is identical with the upper supersaturation level for Zr-Nb alloys at 573 K (300°C) established by Erickson [11,19]. The formation of the solid hydride layer as a result of the high hydrogen ingress rate (which is much higher than the critical rate for the formation of uniform hydride) and the hydrogen content of the core are consistent with the situation expected when the corrosion medium supplies a sufficient hydrogen potential for spontaneous nucleation and growth of hydride to occur at the surface [4].

The Zr-2.5 wt% Nb alloy behaved in essentially the same way as the Zircaloys exposed to LiOH, and formed a diffuse edge to the solid hydride layer. Zr-2.5 wt% Nb is known to reach high uniform hydride levels during long-term corrosion tests [16], as shown by Hillner et al. for Zircaloy [7]. This eliminates the argument of Meyer and Simpson [20] that such an effect would be prohibited in this case by the phase rule, because Zr-2.5% Nb is already a two-phase ($\alpha+\beta$) alloy.

The thermal cycle from 573-473 K (300-200°C) was more effective than that from 573-523 K (300-250°C) in redistributing the solid hydride layer since 336 of the former cycles resulted in a higher core concentration ($\sim$ 350 µg/g) than either 672 or 2688 of the latter cycles. Little difference was seen between the core hydrogen concentration for 672 and 2688 cycles from 573 to 523 K (300 to 250°C), especially in the area well away from the boundary of the nickel-plated area. This suggests that an upper limit to the amount of hydrogen redistribution is reached after a number of cycles $\leq$ 672. The greater effectiveness of the larger temperature cycle in causing supercharging must result from the greater supercooling, since the time at temperature (Figure 1) was less for the 573-473 K (300-200°C) cycle than for the 573-523 K (300-250°C) cycle.

The lengths of time at (or near) 573 K (300°C), $\sim$ 50 minutes for the 573-473 K (300-200°C) cycle and $\sim$ 75 minutes for the 573-523 K (300-250°C) cycle, are within the range where the supercharging should be relatively insensitive to the time at temperature according to Westlake's results [6], and are in the wrong direction to explain the different efficiencies. Since the rate of cooling was identical for both cycles, and slow (6.6 K/min) compared with the rapid quenches found to be necessary for significant reductions in the rate of supercharging [6], it must be the extent of subcooling which makes the larger temperature cycle the more effective. Erickson [19] found that during cooling the amount of hydride precipitated was insufficient to reduce the hydrogen content in solution to the equilibrium solubility (i.e. some supersaturation remained), and that precipitation took place discontinuously as supersaturation built up again to a new level sufficient to nucleate fresh precipitation. Thus, if the 573-523 K (300-250°C) cycle were sufficient to nucleate only one cycle of precipitation, and the 573-473 K (300-200°C) cycle nucleated two successive approximately equal cycles, the amount of supercharging per cycle would be approximately twice as big for the larger cycle, in rough agreement with observation.

The observation of an upper limit to the redistribution suggests that the kinetics of supercharging are not cubic as postulated by Westlake and Ockers [6] but asymptotic. Since Westerman and Westlake used far fewer thermal cycles (max.160) than in these experiments they may not have been able to distinguish between the two possibilities. Most of the previous work has been done with an

upper temperature near 673 K (400°C), and hence a much larger solubility than in these studies. Only the early work of Westerman [2] used an upper temperature of 573 K (300°C). In these experiments, very little supercharging of Zircaloy-2 was achieved for a slow cycle down to room temperature. The reason for the small effect seen in Westerman's initial experiments is unknown, and contrasts with the large effects he observed at ∿ 673 K (400°C).

The reason for the saturation of the supercharging effect at a concentration which appears to be related to the size of the thermal cycle cannot be deduced on the basis of the relatively small number of experiments performed here. It does not appear to be related to the solubility of the metastable γ-ZrH. This is quoted as 160 μg/g (at 573 K) by Asher and Trowse [21], but could be inferred to lie between the "heating" and "cooling" curves for δZrH_x if precipitation of γZrH is the cause of the incomplete equilibration during precipitation in Erickson's work [19]. This would place the solubility of γZrH at 90-100 μg/g (at 573 K). The supersaturations achieved in all our thermal-cycling experiments exceed the higher value for the solubility of γ-ZrH [21]. It seems more probable that the saturation of the supercharging effect is caused by the development of an equilibrium dislocation structure as a result of repeated partial dissolution and precipitation of the hydride. The high density of dislocations around the precipitates could then result in saturation of the effect if partial dissolution of the precipitates became as rapid (in the local stress field of the dislocations) as dissolution and diffusion from the solid hydride rim, because the gradient of supersaturation would then vanish.

(b) In the unplated area:

If the hydrogen contents in the unplated areas of the specimens are plotted, after subtraction of the initial hydrogen content and the amounts of hydrogen absorbed uniformly during corrosion in both LiOH and air (Figure 10), the following conclusions can be drawn:-

(i) After autoclaving in LiOH the distance the hydrogen has diffused along the tube (away from the plated area) is roughly equal to that expected [21] from the diffusion coefficient at 573 K (300°C) and the time in LiOH (5 days).

(ii) After thermal cycling, the maximum diffusion distance along the tube continues to agree with that expected from the total time at temperature.

(iii) There appears to be little or no transfer of hydrogen from the plated region to the unplated region. The areas under the curves in Figure 10 are little changed.

(iv) Immediately after autoclaving the hydrogen concentration in the centre of the specimen at the edge of the nickel plating was close to the γ-ZrH solubility (based on Erickson's [19] results), but much less than the supersaturation limit achieved under the nickel plating by thermal cycling. After the largest number of cycles the hydrogen content at the boundary of the nickel plate had declined to a figure close to the equilibrium terminal solid solubility at 573 K (300°C), which is about 70 ± 10 ppm [22,23].

(v) Virtually no movement occurred of the position of the +hydride boundary at 573 K (300°C).

4.3 Comparison of Metallographic and Analytical Results

The metallographic estimates of hydrogen contents (Figure 5), from the volume fraction of hydride, show much more scatter than the analytical results, possibly because the Metals Research Ltd. QUANTIMET, Quantitative Television Microscope (QTM) cannot distinguish hydride from some other structural features of the polished and etched specimens. However, any variation resulting from such factors should take the form either of a constant factorial error (i.e. the correlation factor between metallographic and analytical contents is unique but differs from that expected theoretically), or of a constant to be subtracted from all the data (i.e. the QTM adds on some constant volume fraction of the specimen because it also counts the volume fraction of etched grain boundaries or the β-Zr/Nb phase).

Traditionally, estimates of the hydrogen contents of zirconium alloys metallographically have been regarded as unreliable, although for carefully controlled experiments in specimens with equiaxed grain structures and relatively low hydrogen contents quite accurate results have been achieved by comparison with standard micrographs rather than by estimation of hydride volume [24]. Examination of our results shows that a good correlation between the metallographic and analytical results cannot be obtained using a single correlation factor in all areas of the specimen. Theoretically, allowing for a density change of ∿ 10%, 100 μg/g hydrogen in zirconium should give ∿ 1 vol% of γ-ZrH or ∿ 0.6 vol% of δ-$ZrH_{1.6}$ To get the best correlation with the background hydrogen contents (beyond the diffusion gradient) in our specimens required a correlation factor of 100 μg/g ≃ 5 vol% zirconium hydride. It is clear that this factor is much larger than that predicted theoretically. It is also evident from the two specimens examined after autoclaving (#1 and #3) that large differences arise between the results of two nominally similar specimens. These differences are much larger than the scatter on results from either specimen. Thus, it seems probable that both the high correlation factor needed to fit the analytical and metallographic results, and the

scatter between similar sections of the same sample, arise from variability in the etching procedure needed to show up the hydride for metallography. The low volume fractions estimated in the low hydrogen areas show that any volume fraction of grain boundaries or second phase being counted by the QTM is very small. The large differences in the appearance of hydride platelets which could arise from minor variations in etching procedure were noted many years ago [25].

Allowing for the possible variations in etching procedure from specimen to specimen, however, the general agreement between analysis and metallography in the low hydrogen areas of all specimens is reasonable (using a correlation factor of 100 μg/g ≡ 5 vol%). Along the length of any one specimen, though, the fit should remain good using a single correlation factor. This is not the case. At high hydrogen contents a correlation factor, which fits the low hydrogen content end of the specimen, underestimates the volume fraction of hydride seen at the high concentration end, except for the specimens given no thermal cycles after autoclaving. To fit the high hydrogen content ends of the other specimens requires a correlation factor 1.5 to 2.0 times higher than at the low concentration end. This suggests that there may be a difference in the composition of the hydrides precipitated in different parts of the same specimen.

Erickson [19] has suggested that the first hydride phase to precipitate on cooling is the metastable γ-ZrH and that this accounts for the failure of the hydrogen concentration in solid solution to drop to the equilibrium solubility for δ-ZrH_x when precipitation starts in a super-cooled specimen. This γ-ZrH is then thought to transform to δ-ZrH_x during heating, in order to account for the same specimen following the equilibrium line during the next heating part of a cycle. If this is so, then the hydrides in the specimen after autoclaving and in the low hydrogen ends of the other specimens will never have seen any thermal cycles, since they will have precipitated only during the final cool down before metallography. Thus, these hydrides could have a different composition from those which have persisted at 300°C and have received repeated thermal cycles.

A much better fit to the whole curves (other than the zero cycle curve) can be achieved if two correlation factors are used, one for the parts of the curves below the terminal solubility ($\sim$ 30 μg/g) at $\sim$ 523 K (250°C) [23], and the other for the remainder of the curve. A ratio of 1.6-2.0 between the two correlation factors would give the best results, however, the higher correlation factor would be required for the higher hydrogen regions of the distribution curves. If the necessity for two correlation factors is explained on the basis of different hydride phases being present in the two regions of the specimen, then this requires the thermally cycled hydrides to be γZrH, and the freshly precipitated hydrides to be δ-ZrH_x ($x = 1.6$ to 2.0).

Studies of the precipitation of zirconium hydride phases [26-28] show that γZrH is formed at cooling rates ≥ 10 K/min, and during precipitation at elevated temperatures when large supersaturations are involved. In our experiments the rate of cooling of the loop system after corrosion in LiOH was probably ≪ 10 K/min, which should result in δZrH_x formation. The rate of cooling during thermal cycling (6.6 K/min), and the degree of supersaturation achieved may just be enough to precipitate γ-ZrH [26]. During the final cooling of the furnace, as the cooling rate falls below 3.5 K/min, at temperatures below 473 K, the final precipitation may be as δ-ZrH_x. The precipitation of γ-ZrH in the centre of the area under the nickel plate during thermal cycling may also have been influenced by the presence of the solid γ-ZrH layer at the plated surface, rather than the expected δ-ZrH_x layer [29]. Although immediately after autoclaving all the hydride precipitated during cooling appears more likely to have been δ-ZrH_x, even under areas carrying a solid layer of γ-ZrH.

The recent suggestion of Cann and Atrens [30], that γ-ZrH is the preponderant phase precipitated below ∿ 700 K (423°C) and the only phase precipitated below ∿ 525 K (252°C)(i.e. for specimens with hydrogen contents ≤ 230 μg/g and 21 μg/g, respectively), does not agree with our observations. However, these authors were studying only intragranular hydrides in large grained zirconium; a situation very different from the hydride morphology in this work.

5. CONCLUSIONS

The thermal cycling experiments reported here lead to the following conclusions:

(i) Hydrogen absorption by nickel-plated Zr-2.5% Nb alloy specimens in concentrated LiOH solution at 573 K (300°C) is an erratic process. The variability of the hydrogen absorption can be understood best if the source of the hydrogen is cathodic hydrogen generated at the nickel-plating surface by the galvanic couple with Zr-Nb, and if the galvanic current is controlled by the anodic reaction (i.e. the anodic area exposed to the LiOH is controlling).

(ii) The distribution of hydrogen in the nickel-plated area after corrosion agrees with Marino's hypothesis [4] for supercharging, and in this experiment the hydrogen concentration in the core of the nickel-plated area was equal to the upper limit of supersaturation (i.e. ∿130 ppm) for 573 K (300°C). The formation of a diffuse hydride layer adjacent to the solid hydride was not inhibited by the two-phase (α+β)-Zr nature of the alloy.

(iii) Further supercharging during thermal cycling is possible via the Westlake and Ockers [6] mechanism.

(iv) The extent of supercharging was increased by increasing supercooling of the specimens over the range 300 to 200°C, and little affected by the time at the upper temperature, provided this exceeded $\sim$ 50 minutes.

(v) The rate of diffusion of the hydrogen (in solid solution) along the tube was in agreement with predictions from the diffusion coefficient for hydrogen in zirconium at 300°C.

(vi) The solid hydride layer formed beneath the nickel-plating appears to be γ-ZrH and not the expected δ-ZrH_x.

(vii) The precipitated hydrides in the centre of the nickel-plated area after thermal cycling seem more likely to be γ-ZrH than δ-ZrH_x, although immediately after autoclaving they may be δ-ZrH_x. In the rest of the specimen, the best fit to the data is achieved if they are δ-ZrH_x.

(viii) No significant transfer of hydrogen from the α+hydride to the α-region (at 300°C) was observed.

(ix) The α+hydride phase boundary will not migrate along a pressure tube as a result of thermal cycling (up to 2688 cycles) between 300 and 250°C.

References

[1] A. Sawatzky, J. Nucl. Mat., 1960, 2, 321.

[2] R.E. Westerman, "On Charging α-Phase Zircaloy-2 with Hydrogen Beyond the Solubility Limit - Interim Report", U.S. Report HW-73382, April 1962.

[3] R.E. Westerman, J. Nucl. Mat., 1966, 18, 31.

[4] G.P. Marino, U.S. Report WAPD-T-2303, Aug. 1969, and Mat. Sci. and Eng., 1971, 7, 335.

[5] G.P. Marino, "Hydrogen Behaviour in Zirconium Based Alloys" U.S. Report WAPD-TM-759, June 1968.

[6] D.G. Westlake and S.T. Ockers, J. Nucl. Mat., 1970, 37, 236.

[7] E. Hillner, J.N. Kass and J.J. Kearns, J. Nucl. Mat., 1972/73, 45, 175.

[8] R.A. Murgatroyd and J. Winton, U.K.A.E.A. Report TRG 1439(C) 1967, and J. Nucl. Mat., 1967, 23, 249.

[9] J. Winton and M. Farrow, "Gas Hydriding Zircaloy-2 at 400°C", U.K.A.E.A. Report TRG-1446(C), 1967.

[10] S. Kass, U.S. Report WAPD-TM-656, Nov.1967, and Corrosion, 1969, 25, 30.

[11] W.H. Erickson and D. Hardie, J. Nucl. Mat., 1964, 13, 254.

[12] C.R. Cupp and P. Flubacher, J. Nucl. Mat., 1962, 6, 213.

[13] C.E. Ells, Can. Met. Quart. 1978, 17, 32.

[14] E.G. Price, Can. Met. Quart. 1972, 11, 129.

[15] H. Coriou, L. Grall, J. Meunier, M. Pelras and H. Willermoz, J. Nucl. Mat., 1962, 7, 320.

[16] B. Cox and J.A. Read, "Oxidation of a Zr-2½% Nb Alloy in Steam and Air", U.K.A.E.A. Report AERE-R4459, October 1963.

[17] C.E. Ells, Atomic Energy of Canada Limited, Chalk River, unpublished results.

[18] C.E. Coleman, ibid.

[19] W.H. Erickson, Electrochem. Tech., 1966, 6, 205.

[20] P. Mayer and C.J. Simpson, Proceedings of 2nd Int. Conf. on Hydrogen in Metals, Paris, 1978, Paper 1D5.

[21] R.C. Asher and F.W. Trowse, J. Nucl. Mat., 1970, 35, 115.

[22] J.J. Kearns, J. Nucl. Mat., 1967, 22, 292.

[23] C.E. Coleman and J.F.R. Ambler, Can. Met. Quart., 1978, 17, 81.

[24] L.A. Hartcorn and R.E. Westerman, "Quantitative Metallography of Hydride Phase in Zircaloy-2 Process Tubes", U.S. Report, HW74949, Nov. 1963.

[25] B. Cox and T. Johnston, "Some Observations of Hydride in Zirconium and Zircaloy-2 and its Subsequent Effect on Corrosion", U.K.A.E.A. Report, AERE-R3881, January 1962.

[26] J.S. Bradbrook, G.W. Lorimer and N. Ridley, J. Nucl. Mat., 1972, 42, 142.

[27] G.J.C. Carpenter, Acta Met., 1978, 26, 1225.

[28] J. Pegoud and J. Guillaumin, J. Nucl. Mat., 1972, 45, 69.

[29] B. Cox and V.C. Ling, Atomic Energy of Canada Limited, Progress Report AECL-6966 (1980), p.71.

[30] C.D. Cann and A. Atrens, J. Nucl. Mat., 1980, 88, and Atomic Energy of Canada Limited, Report AECL-5996 (May 1978).

TABLE 1: METALLOGRAPHIC ESTIMATES OF VOLUME FRACTION OF ZIRCONIUM HYDRIDE ALONG THE CENTRE-LINE OF EACH SPECIMEN

Distance from End of Ni Plate (cm)	After Autoclaving (%)		After 336 Cycles 300-200°C (%)	After 672 Cycles 300-250°C (%)	After 2688 Cycles 300-250°C (%)
Specimen No.:-	#1	#3	#2	#3	#4
4.0	-	-	-	-	22.75
3.0	-	6.56	-	20.18	13.89
2.0	-	3.38	-	15.42	16.28
1.0	-	4.51	-	17.32	17.61
0.5	-	-	23.81	-	-
0.25	-	-	19.17	-	-
0	3.45	;6.09	9.54	14.84	8.49
0.25	-	-	14.26	-	-
0.5	-	-	4.32	-	-
1.0	0.871	;4.48	2.51	8.67	4.23
1.5	-	-	3.56	-	-
1.75	-	-	1.37	-	-
2.0	0.851	;1.65	0.795	3.03	4.15
2.5	-	-	0.975	-	-
3.0	0.610	;0.757	0.690	2.22	3.69
4.0	0.634	;0.768	0.440	3.01	3.39
5.0	-	0.481	-	1.03	3.29
6.0	-	0.376	-	1.12	2.77
7.0	-	0.448	-	1.08	2.86
Mean of last 3 points	-	0.435	0.440	1.08	2.97
Final H Analyses from Table 2 Converted by Factor 100 ppm ≈ 5 vol%	-	0.405	0.671	1.20	1.73
H Content at Boundary of Ni Plate (Converted Using the Same Factor)	-	5.05	7.0	5.5	4.0
Peak H Content Beneath Ni Plate (Using Same Factor)	-	7.0	17.75	13.5	11.75

TABLE 2: HYDROGEN ANALYSES OF THERMALLY CYCLED Zr-2.5% Nb SPECIMENS

Distance from End of Ni Plate (cm)	Specimen Desig.	After Autoclaving (ppm)	After 336 Cycles 200-300°C (ppm)	After 672 Cycles 250-300°C (ppm)	After 2688 Cycles 250-300°C (ppm)
5.00					
4.75	T*	-	231		
4.50	S	314	178	165	158
4.25	R*	664	483	165	
4.00	Q	119	205	202	172
3.75	P*	895	886	385	210
3.50	O	126	217	210	185
3.25	N*	862	1300	501	399
3.00	M	143	253	213	205
2.75	L*	473	1245	790	346
2.50	K	137	338	252	239
2.25	J*	1207	1368	1026	452
2.00	I	142	346	270	212
1.75	H*	1090	1433	1087	225
1.50	G	122	363	202	232
1.25	F*	789	1410	850	192
1.00	E	126	317	318	139
0.75	D*	1052	1379	806	108
0.50	C	133	294	225	88
0.25	B*	738	1132	760	77
0	A	101	220	104	80
0.25	1	102	106	(180)	70
0.50	2	69	85	(95)	64
0.75	3	77	52	(122)	69
1.00	4	(96)	49	73	67
1.25	5	39	45	51	62
1.50	6	29	38	51	63
1.75	7	19	32	47	55
2.00	8	23	33	46	55
2.25	9	13	25	47	(68)
2.50	10	13	25	43	55
2.75	11	8	24	40	47
3.00	12	8	20	38	54
3.25	13	15	18	35	51
3.50	14	(42)	(34)	35	50
3.75	15	(117)	19	34	48
4.00	16	8	15	34	49
4.25	17	5	12	30	47
4.50	18	8	14	30	48
4.75	19	10	18	29	46
5.00	20	7	9	26	40
5.25	21	9	(34)	25	38
5.50	22	(168)	16	23	[illegible]
5.75	23	(121)	17	24	36
6.00	24	10	8	22	34
6.25	25				30
6.50	26				35
6.75	27				37
7.00	28				31
Average of last analyses (No. used)		8.14(7)	13.43(7)	24.0 (5)	34.6 (5)
Hydrogen uptake† in Each Experiment		3.54 (5 days)	5.29 (21 days)	15.86 (42 days)	26.46 (168 days)

*Alternate specimens in Ni-plated area had the solid hydride layer ground off before analysis. Asterisks show specimens including solid hydride.

†Original hydrogen content analyzed as 7, 7, 5, 2, 2 ppm; mean 4.6 ppm.

( )Specimens apparently contaminated with incompletely dissolved bio-plastic, give high results. Lesser contamination of other specimens may be present but undetected. Specimens showed traces of organic contamination during mass spectrometer analysis.

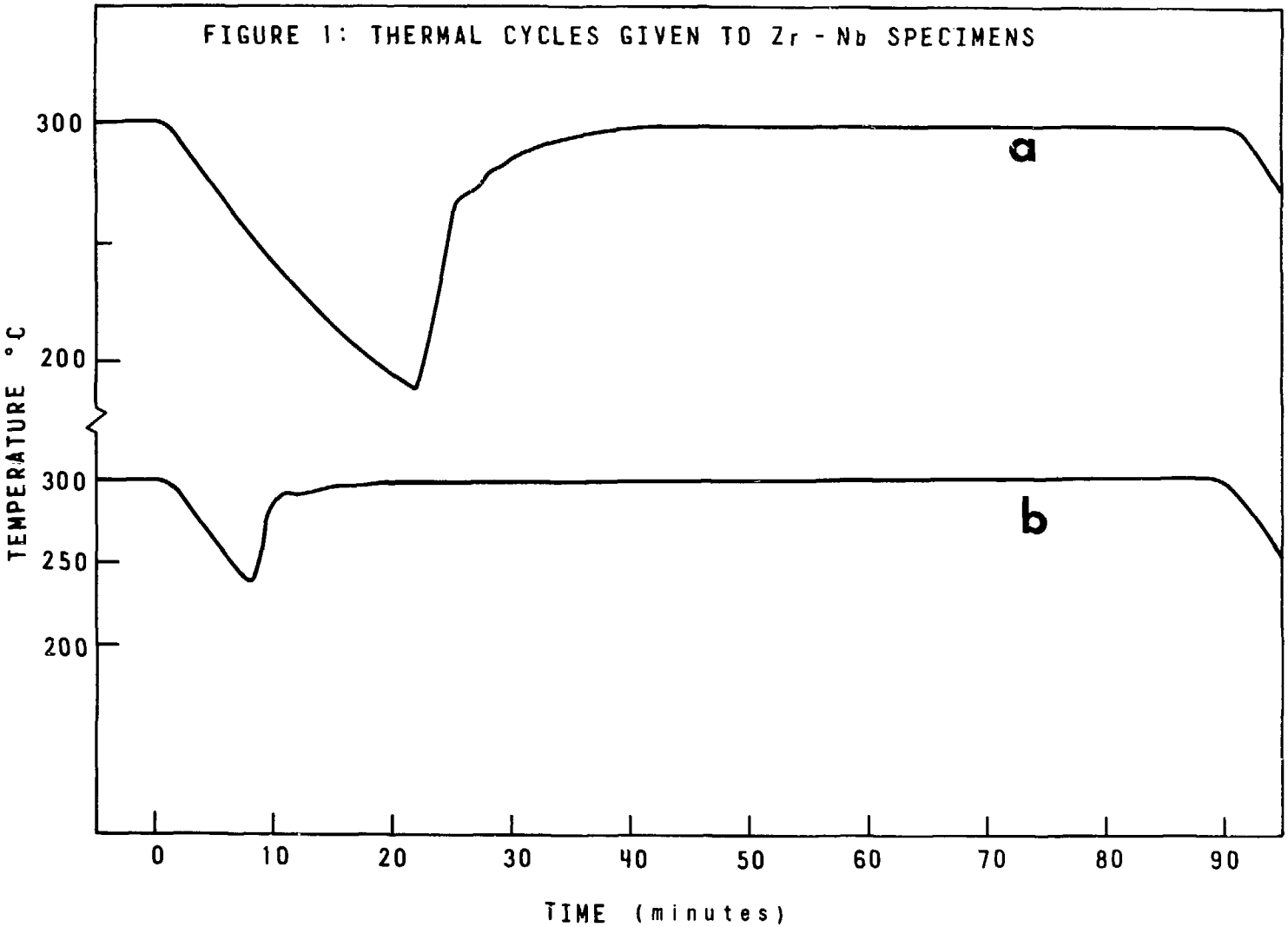
FIGURE 1: THERMAL CYCLES GIVEN TO Zr - Nb SPECIMENS
300
200
300
250
200
TEMPERATURE °C
a
b
0
10
20
30
40
50
60
70
80
90
TIME (minutes)

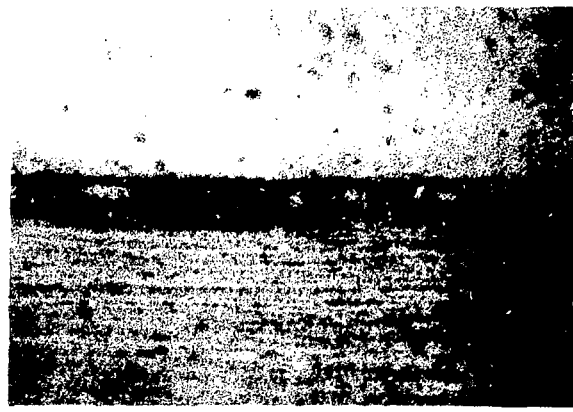

a. Uniform friable oxide on pressure tube (x1000)

b. Thick compact oxide on specimen end (x1000)

Figure 2

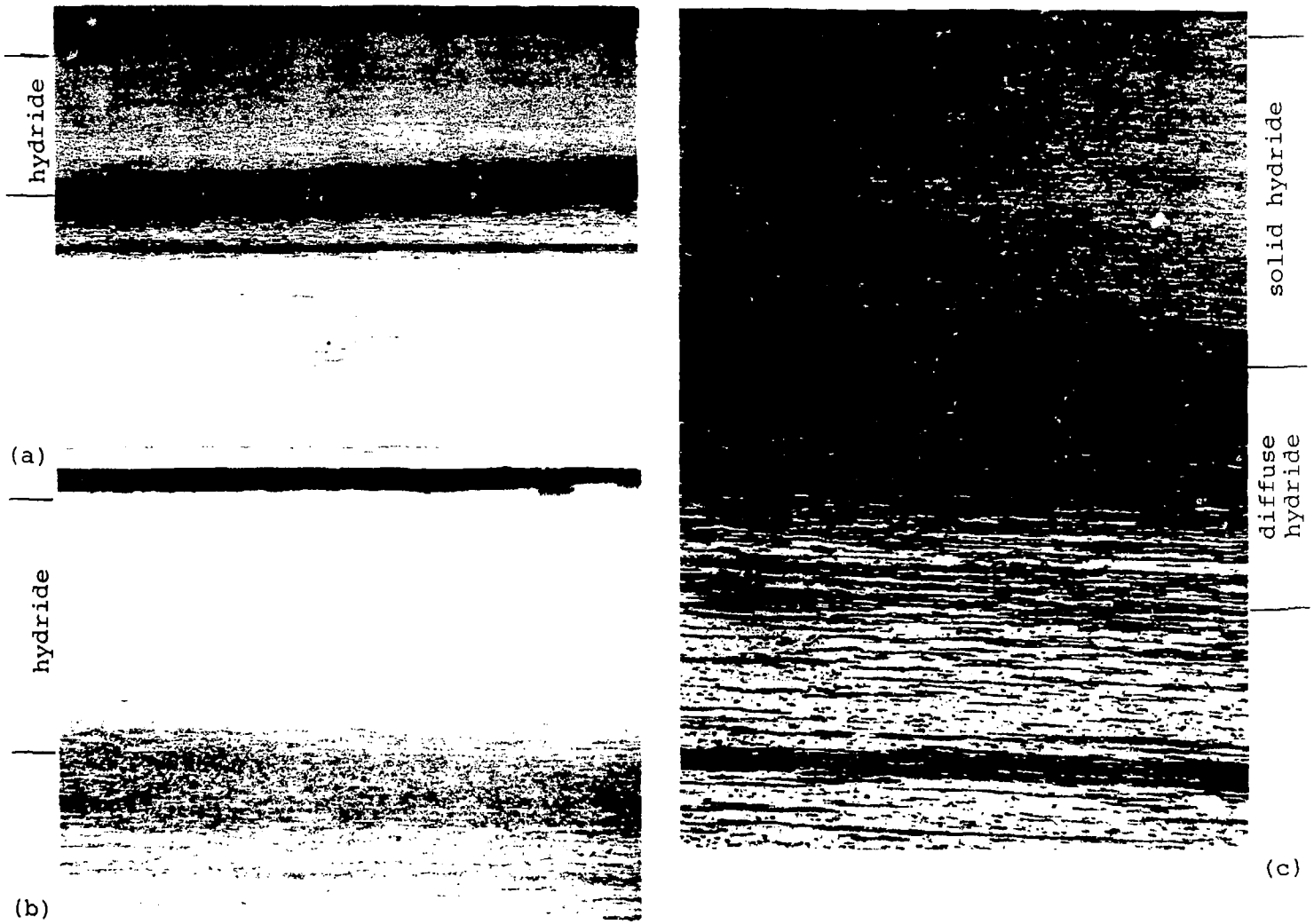

Figure 3 Hydride redistribution beneath Ni-plating after 5 days in 300°C LiOH. (a) x40, (b) and (c) x100. Note appearance of original CW Zr-Nb structure in hydride in (c).

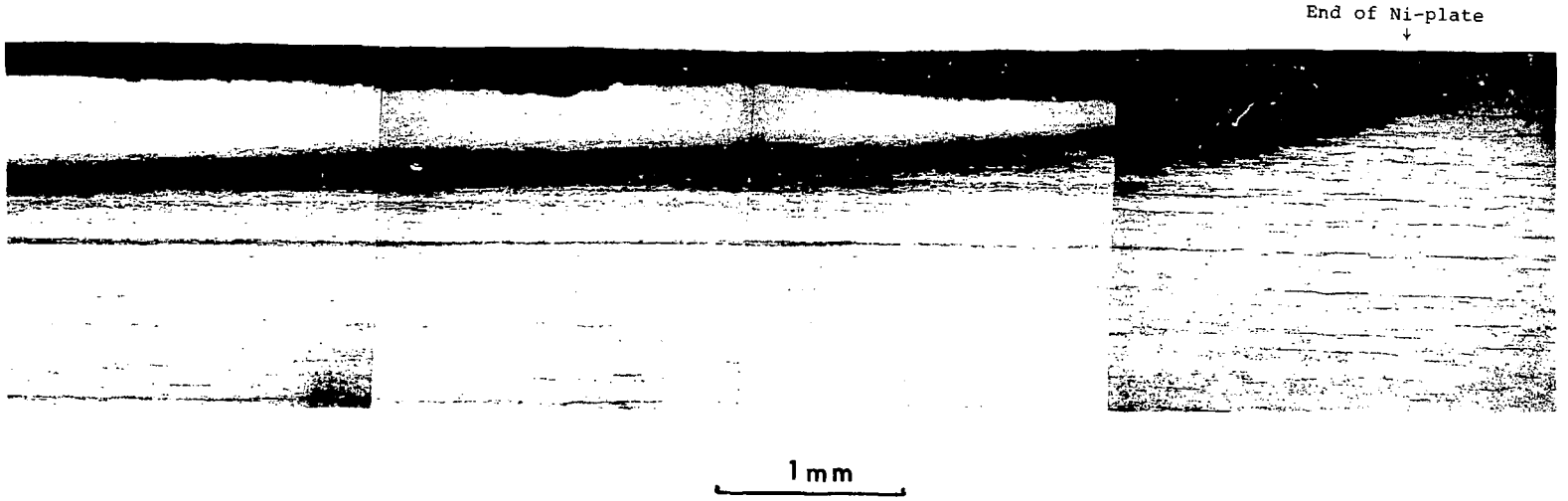

Figure 4 Solid hydride layer, with diffuse hydride zone immediately beneath it, terminating at the end of the nickel-plated area. Note tendency of diffuse hydride to layering parallel to the CW Zr-2.5% Nb alloy structure.

FIGURE 5 METALLOGRAPHIC ESTIMATES OF VOLUME FRACTION OF ZIRCONIUM BY HYDRIDE

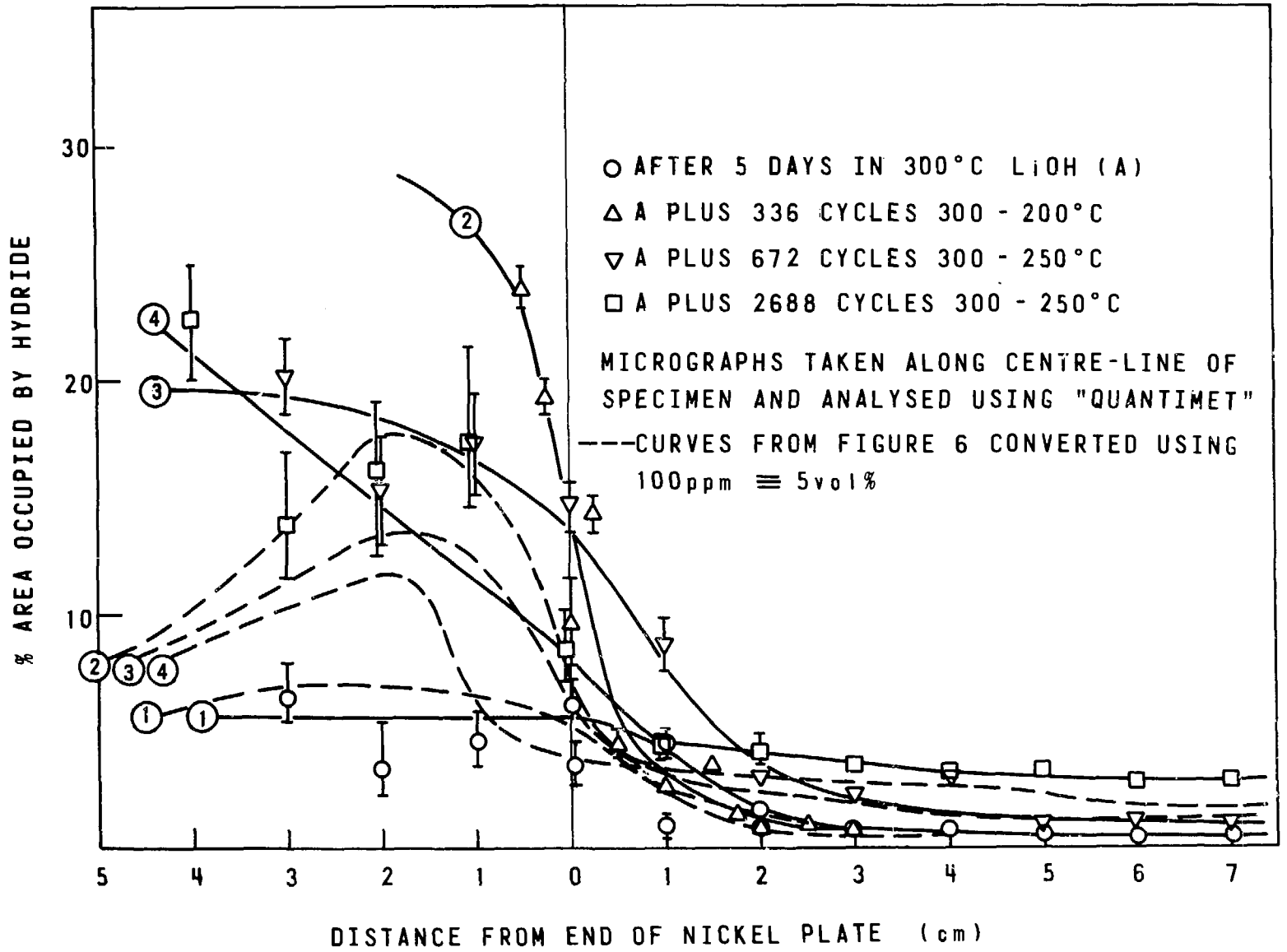

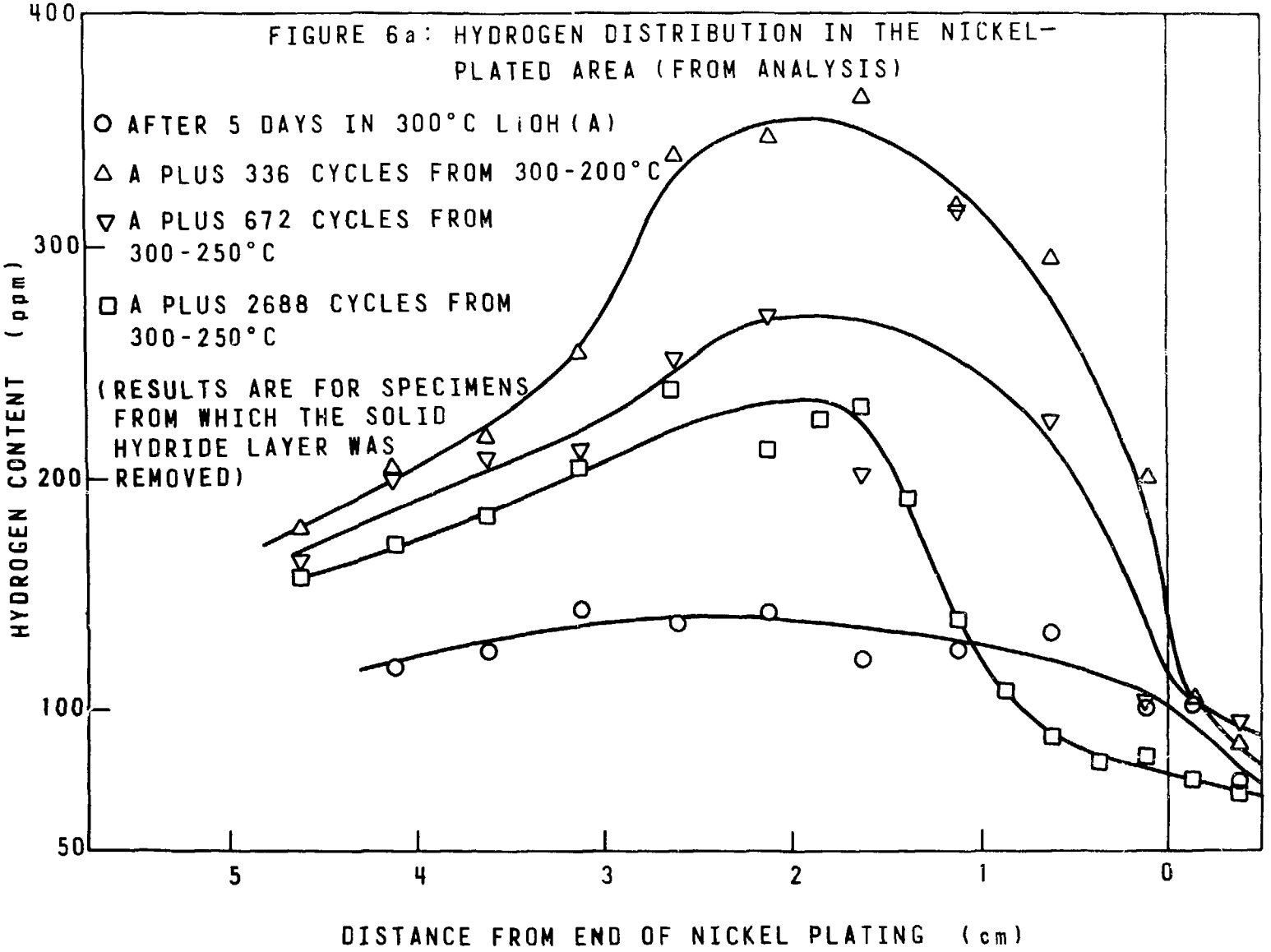
FIGURE 6a: HYDROGEN DISTRIBUTION IN THE NICKEL-PLATED AREA (FROM ANALYSIS)
O AFTER 5 DAYS IN 300°C LiOH (A)
△ A PLUS 336 CYCLES FROM 300-200°C
▽ A PLUS 672 CYCLES FROM 300-250°C
□ A PLUS 2688 CYCLES FROM 300-250°C
(RESULTS ARE FOR SPECIMENS FROM WHICH THE SOLID HYDRIDE LAYER WAS REMOVED)
HYDROGEN CONTENT (ppm)
400
300
200
100
50
5
4
3
2
1
0
DISTANCE FROM END OF NICKEL PLATING (cm)

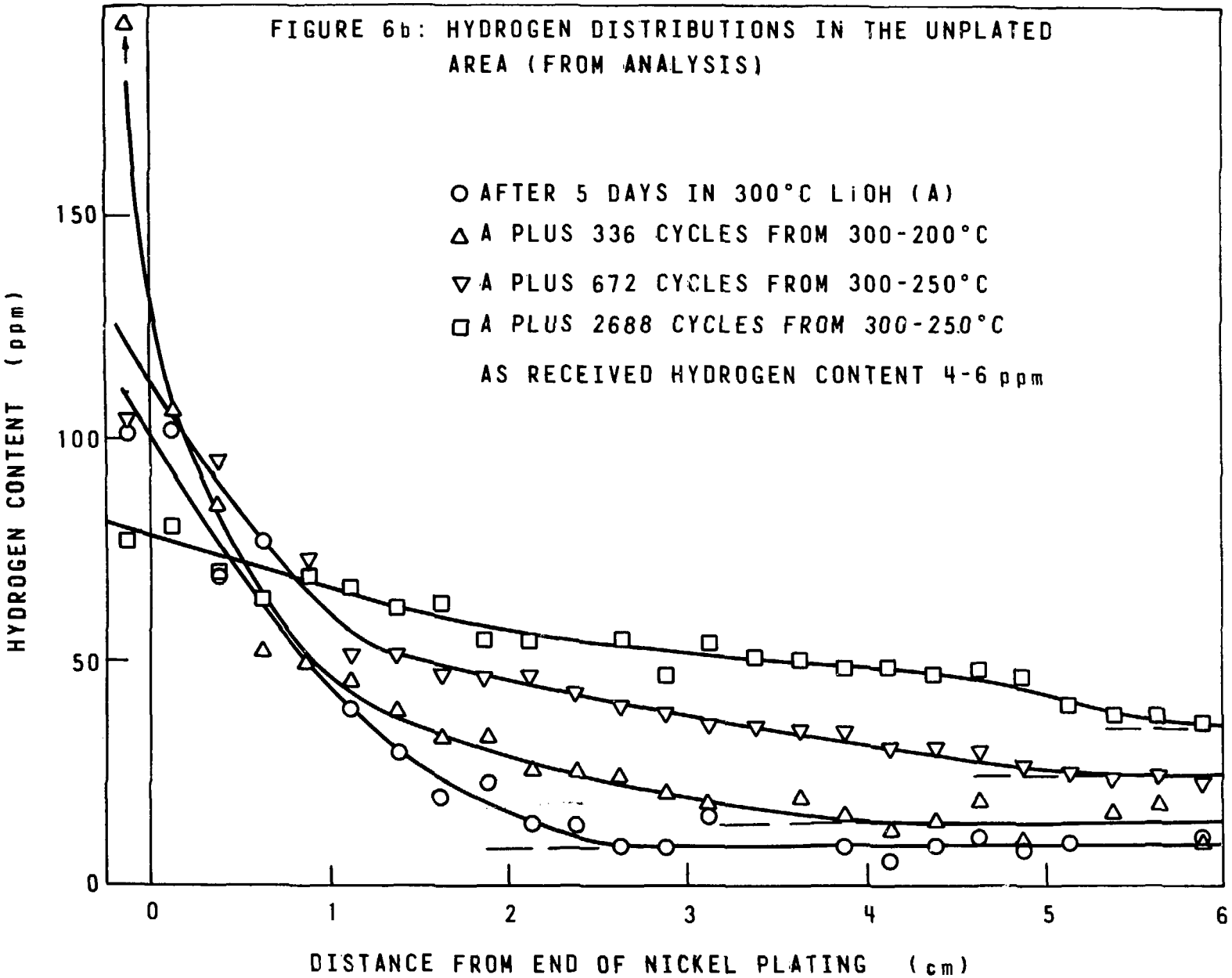
FIGURE 6b: HYDROGEN DISTRIBUTIONS IN THE UNPLATED AREA (FROM ANALYSIS)
○ AFTER 5 DAYS IN 300°C LiOH (A)
△ A PLUS 336 CYCLES FROM 300-200°C
▽ A PLUS 672 CYCLES FROM 300-250°C
□ A PLUS 2688 CYCLES FROM 300-250°C
AS RECEIVED HYDROGEN CONTENT 4-6 ppm
HYDROGEN CONTENT (ppm)
150
100
50
0
0
1
2
3
4
5
6
DISTANCE FROM END OF NICKEL PLATING (cm)

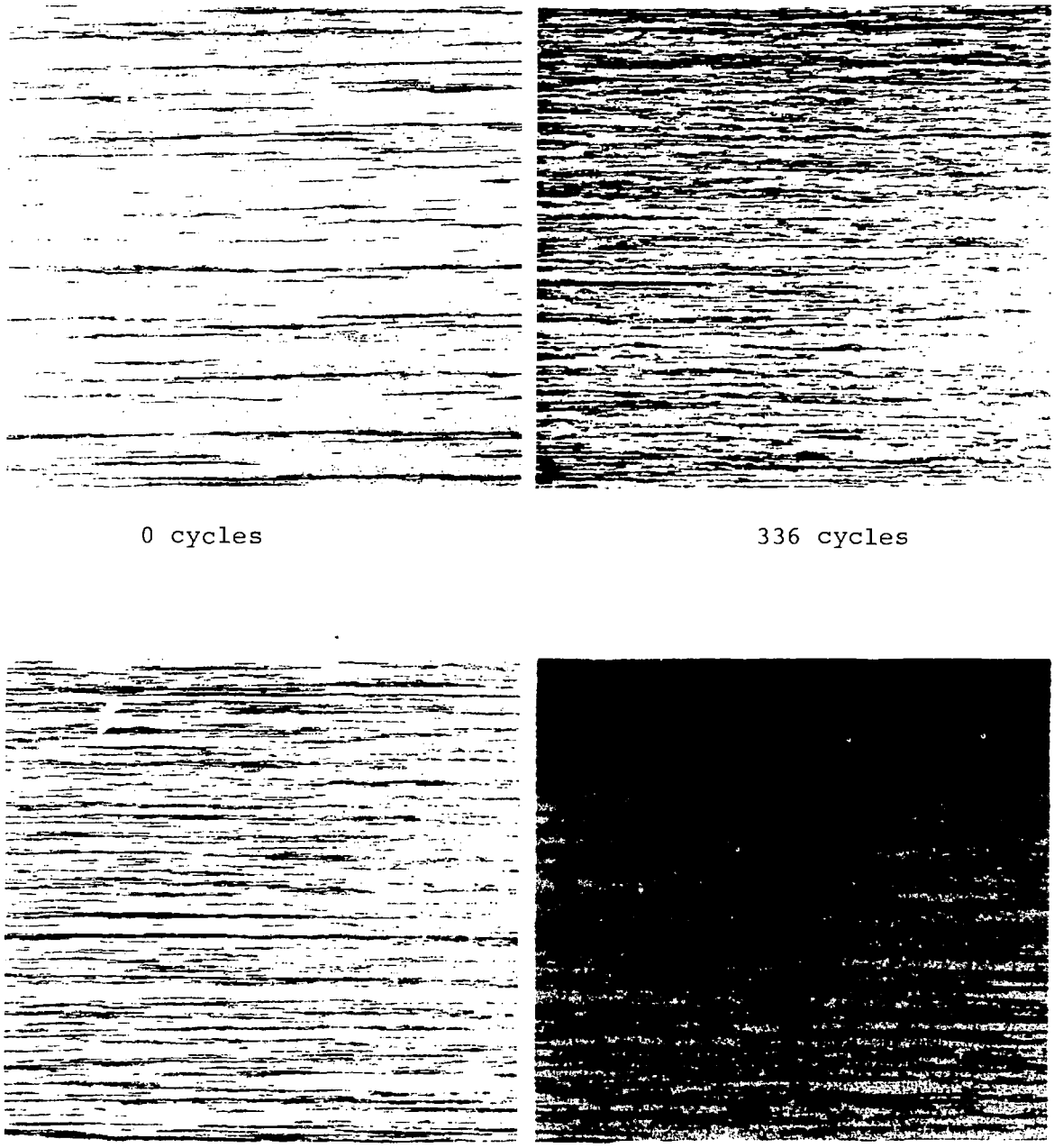

Figure 7 Four specimens compared at the peak hydrogen content in the centre of the specimen beneath the nickel-plated area (x100).

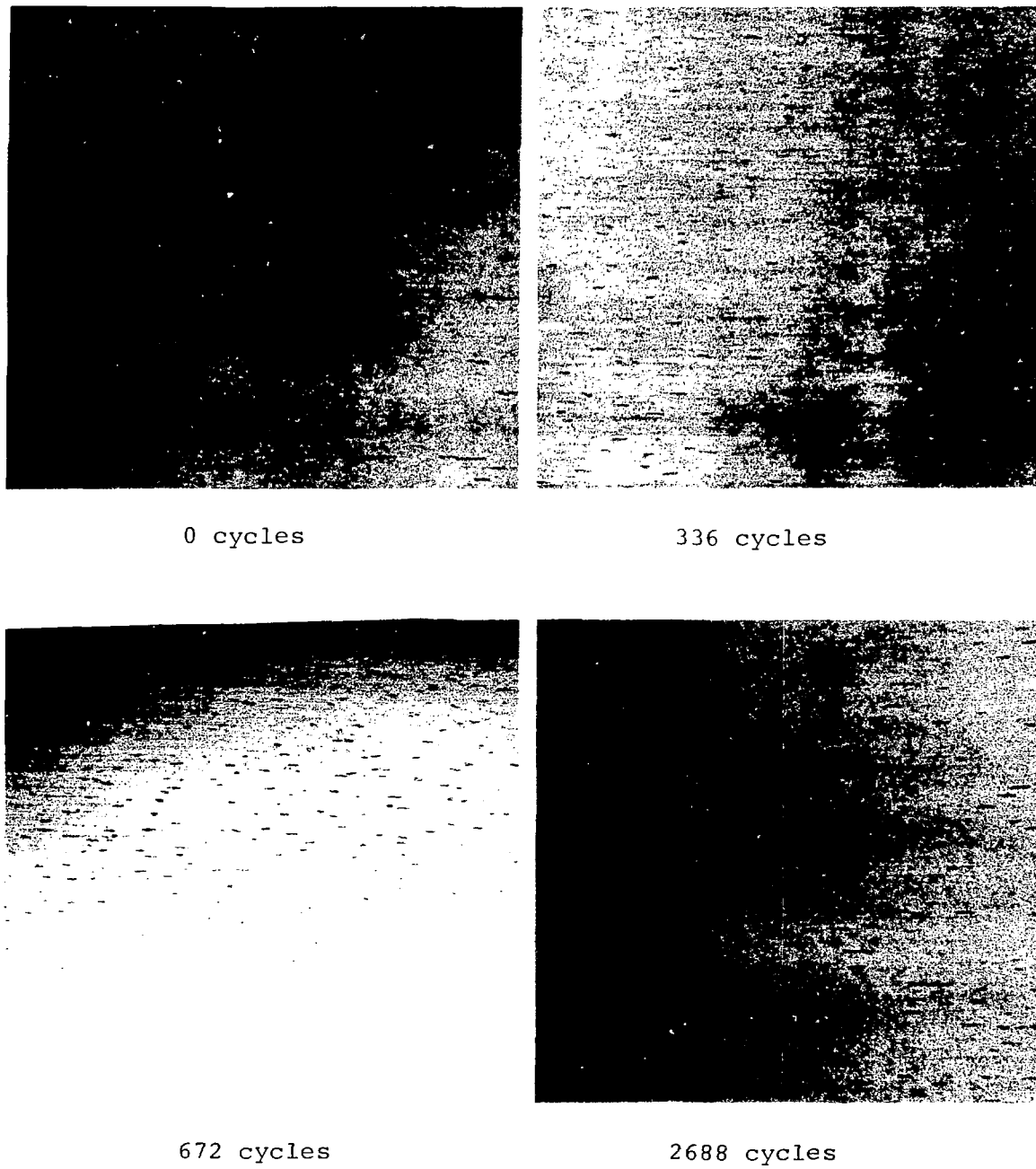

0 cycles

336 cycles

672 cycles

2688 cycles

Figure 8 Four specimens compared at a point beyond the hydrogen diffusion profile in each specimen. Note that individual hydride plates are smaller after cycling than before cycling because of the slower cooling rate of the autoclaves (x100).

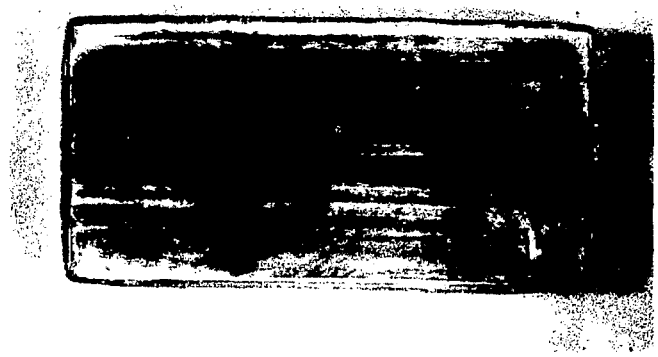

(a) x2

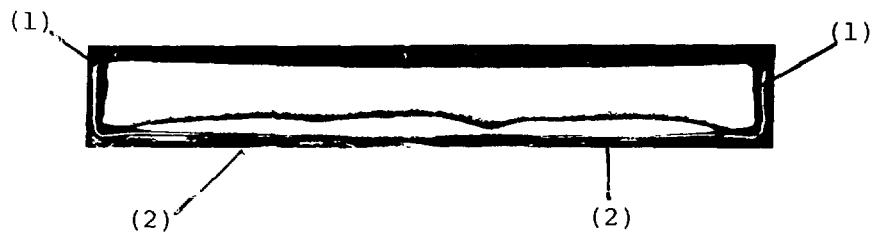

(b) x5

Figure 9 One of the small specimens exposed to LiOH at the same time as the specimen for thermal-cycling studies. Note:-

(a) Streaky nature of white oxide and prevalence of white oxide along edges on unplated face.

(b) Poor adherence of nickel plate at edges (1) and good adherence at a few sites on the surface (2), leading to uneven distribution of solid hydride in this transverse section.

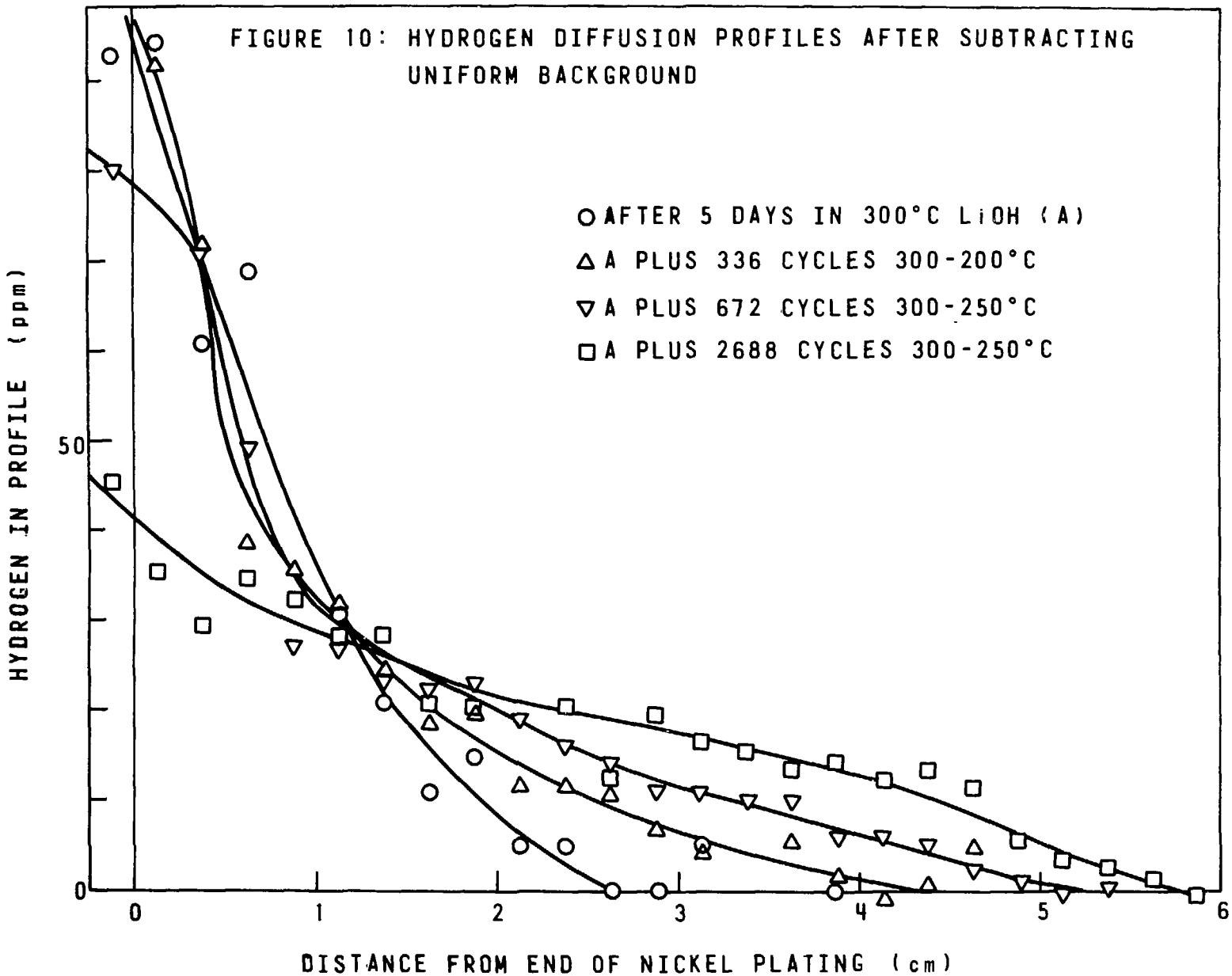
FIGURE 10: HYDROGEN DIFFUSION PROFILES AFTER SUBTRACTING UNIFORM BACKGROUND
○ AFTER 5 DAYS IN 300°C LiOH (A)
△ A PLUS 336 CYCLES 300-200°C
▽ A PLUS 672 CYCLES 300-250°C
□ A PLUS 2688 CYCLES 300-250°C
HYDROGEN IN PROFILE (ppm)
50
0
0
1
2
3
4
5
6
DISTANCE FROM END OF NICKEL PLATING (cm)

ISSN 0067 - 0367

To identify individual documents in the series we have assigned an AECL- number to each.

Please refer to the AECL- number when requesting additional copies of this document

from

Scientific Document Distribution Office
Atomic Energy of Canada Limited
Chalk River, Ontario, Canada
K0J 1J0

Price $3.00 per copy

ISSN 0067 - 0367

Pour identifier les rapports individuels faisant partie de cette série nous avons assigné un numéro AECL- à chacun.

Veuillez faire mention du numéro AECL- si vous demandez d'autres exemplaires de ce rapport

au

Service de Distribution des Documents Officiels
L'Energie Atomique du Canada Limitée
Chalk River, Ontario, Canada
K0J 1J0

Prix $3.00 par exemplaire

1245–80